Ecological Processes

RESEARCH

Open Access

Passivation remediation of weakly alkaline Cd-contaminated soils using combined treatments of biochar and sepiolite

Yuxin Zhang[1,2†], Shan Gao[1†], Hongtao Jia[2], Tao Sun[1], Shunan Zheng[3*], Shihang Wu[1] and Yuebing Sun[1]

Abstract

Background Cadmium (Cd) pollution in agricultural soils has become a priority environmental concern globally. A reasonable application of passivators is critical to address the problem. In this study, we examined the remediation effects of rice husk biochar (rBC) and sepiolite (Sep) as single and combined (rBC + Sep) treatments on Cd pollution in a weakly alkaline soil using three maize cultivars (Liyu 16, Zhengdan 958, and Sanbei 218) as test crops. We also explained the mechanisms involved in the remediation effects.

Results The pseudo-second-order kinetic equation and Langmuir model could well describe the adsorption process of rBC + Sep for Cd^{2+}. Compared with the control treatment (CK), soil available Cd concentration decreased by 29.51–36.34% under rBC + Sep treatment ($p < 0.05$) and the Cd concentrations in maize grains of Liyu 16, Zhengdan 958, and Sanbei 218 decreased by 38.08–47.85%, 37.25–45.61%, and 33.96–46.15%, respectively ($p < 0.05$). Following passivation treatment, soil available Cd concentration decreased and gradually changed from the exchangeable and carbonate binding forms to the Fe/Mn oxide and residual forms. The bioconcentration factors of Liyu 16 (0.05–0.09) and Sanbei 218 (0.05–0.09) were lower than those of Zhengdan 958 (0.07–0.13). In addition, rBC +Sep treatment increased soil pH and soil electrical conductivity, but the differences were not significant ($p > 0.05$).

Conclusions The application of 0.2% rBC + 0.5% Sep composite passivation material to weakly alkaline Cd-contaminated soil can effectively reduce the Cd concentration of soil and maize.

Keywords Cd, Rice husk biochar, Sepiolite, Passivation restoration, Weakly alkaline soil, Maize

Introduction

Soil cadmium (Cd) pollution has become an important problem affecting human health and environmental safety in China and many other patrs of the world (Fan et al. 2020). According to the National Soil Pollution Status Survey Bulletin, in 2014, 7.0% of soils in China exceeded the standard for Cd pollution (Zhao et al. 2015). Statistics indicate that approximately 10 million ha of land in China is contaminated by heavy metals and over 12 million tons of grains are contaminated by heavy metals each year (Zhou et al. 2014; Sun et al. 2017). Cd is a toxic heavy metal that is silver-white in color and has a long half-life, making it difficult to reduce in the environment and easy to migrate and transform. The entry of Cd into the food chain poses a threat to human health (Fan

†Yuxin Zhang and Shan Gao contributed equally to this work and should be considered co-first authors.

*Correspondence:
Shunan Zheng
zhengshunan1234@163.com
[1] Key Laboratory of Original Agro–Environmental Pollution Prevention and Control, Ministry of Agriculture and Rural Affairs (MARA)/Tianjin Key Laboratory of Agro–Environment and Agro–Product Safety, Agro–Environmental Protection Institute, MARA, Tianjin 300191, China
[2] College of Resources and Environment Sciences, Xinjiang Agricultural University, Urumqi 830052, China
[3] Rural Energy and Environment Agency, Ministry of Agriculture and Rural Affairs, Beijing 100125, China

et al. 2020). Therefore, the remediation of Cd pollution in soil environments is urgent.

In recent years, in-situ passivation remediation has emerged as a promising technique for treating contaminated soils because of its high efficiency and low cost. Commonly used passivators include clay minerals and biochar. Biochar is a carbon-rich material produced from biomass under high-temperature and oxygen-limited conditions. The porous structure and oxygen-rich functional groups on the surface of biochar enable the adsorption and passivation of heavy metals through mechanisms such as surface complexation, ion exchange, electrostatic adsorption, and coprecipitation (Ahmad et al. 2014; Xiao et al. 2018; Cheng et al. 2020). Additionally, biochar can be produced from a wide range of raw materials, providing a waste-to-resource solution and enhancing crop yield. Clay minerals possess large pore volumes and specific surface areas and are effective in passivating heavy metal-contaminated soils through adsorption, ion exchange, and co-precipitation, as well as in reducing Cd absorption in crops (Covelo et al. 2007; Song et al. 2011). Both biochar and clay minerals possess excellent adsorption capabilities owing to their unique surface structures, making them highly desirable passivators for the study of soil heavy metal pollution. Zhang et al. (2018) found that a montmorillonite and wheat straw biochar composite was effective in adsorbing norfloxacin from solution through electrostatic interactions, hydrogen bonding, and pore filling. Xie (2020) investigated the adsorption of Pb^{2+} in weakly alkaline soil using a montmorillonite and rice husk biochar (rBC) composite and found that the primary mechanism was chemisorption, with physical adsorption also playing a role. As different passivators exhibit varying degrees of adsorption capacity for heavy metals, the selection of an appropriate passivator has become a key factor in the success of in-situ passivation and remediation.

Sepiolite (Sep) is a natural clay mineral that possesses a unique fibrous porous structure and large surface area, which enables it to adsorb both organic and inorganic ions with good potential for heavy metal adsorption (Abad-Valle et al. 2016). As the pH increases, surface complexation and isomorphous substitution coexist, enhancing its ability to adsorb and passivation heavy metals (Basta and McGowen 2004; Liang et al. 2014). However, studies have shown that when Sep is applied as a single passivation agent, its effect on Cd passivation decreases over time (Zhang et al. 2023).

This study aimed to examine the combined use of rBC and Sep for the prevention and control of Cd pollution in soil. To achieve this, we studied the passivation effects and mechanisms of different compound ratios of rBC and Sep on Cd in a weakly alkaline agricultural soil using three maize cultivars (Liyu 16, Zhengdan 958, and Sanbei 218) as test crops. The results of this study can be used to inform environmental management for Cd and other heavy metal pollution.

Materials and methods

Experimental site

The experimental site was located in a Cd-polluted farmland in Nansunzhuang, Dongli District, Tianjin City (39°09′N, 117°31′E), China, which belongs to the Haihe River Basin and has a temperate semi-humid continental monsoon climate. The average annual precipitation is 643.8 mm, the frost-free period is 237 d, and the average annual temperature is 13.5 °C. The soil is classified as fluvo-aquic soil with a pH of 8.33, electric conductivity (EC) of 256.3 $\mu S \cdot cm^{-1}$, and soil dissolved organic carbon (DOC) of 93.96 $mg \cdot kg^{-1}$. The soil Cd, Pb, As, and Cr concentrations are 1.30, 29.79, 17.41, and 36.67 $mg \cdot kg^{-1}$, respectively.

Material preparation and characterization

The rice husk was air-dried, sieved to remove gravel and debris, and ground using a high-speed universal grinder. The biochar was produced by pyrolyzing the rice husk at 600 °C for 2 h under anaerobic conditions using a continuous carbonization machine. After the pyrolysis, the biochar was cooled to room temperature and stored in bags. The basic chemical properties of the passivation agents are listed in Table 1. The surface morphologies and structural characteristics of the samples were analyzed using a scanning electron microscope (SEM; Hitachi SU3500) equipped with an energy-dispersive spectrometer and a transmission electron microscope (EDS; JEOL JEM2010). The phase compositions and crystal structures of the samples were obtained using X-ray diffraction (XRD; Rigaku D/Max 2500) in the scanning range of 10–90°. Fourier transform infrared spectrophotometer (FTIR; Nicolet 380) was used to determine changes in functional groups, with a measured wavenumber range of 400–4000 cm^{-1} and a resolution of 1 cm^{-1}.

Table 1 Basic chemical properties of amendments

Chemical properties	Rice husk biochar	Sepiolite
pH	9.76	8.95
C (%)	42.07	6.33
N (%)	0.55	Nd
H (%)	3.86	0.26
O (%)	23.27	18.44
Cd ($mg \cdot kg^{-1}$)	Nd	Nd

Not detected (Nd)

Batch adsorption experiment

A total of 1 g of rBC, 1 g of Sep, and a mixture of 0.5 g of rBC and 0.5 g of Sep (rBC + Sep) were separately placed into 500 mL of Cd nitrate solution with an initial concentration of 100 mg·L^{-1} of Cd^{2+}. The solutions were stirred constantly for 24 h at 25 °C and 300 rpm using a magnetic stirrer. Samples were taken at various time intervals (1, 3, 5, 10, 15, 20, 30, 40, 60, 120, 180, 240, 300, 360, 480, 600, 720, and 1440 min) and the Cd^{2+} concentration was measured using inductively coupled plasma mass spectrometry (ICP-MS; iCAP Q, USA) after passing through 0.45-μm filter.

For a series of concentrations of Cd^{2+} (30, 60, 90, 120, 150, and 200 mg·L^{-1}), 0.1 g of the adsorbent was added and the optimal adsorption time was determined by shaking the solution at 180 rpm and 25 °C. The supernatant was filtered through a 0.45-μm filter and the Cd^{2+} concentration was determined using ICP-MS.

Field experiment

In May 2020, a field experiment was conducted to remediate the soil pollution. The experiment consisted of eight treatments, including a control treatment with no application of a remediation agent (CK) and treatments with the application of 0.1% and 0.2% rBC (A1, A2), 0.2% and 0.5% Sep (S1, S2), 0.1% rBC and 0.2% Sep (A1S1), 0.2% rBC and 0.2% Sep (A2S1), and 0.2% rBC and 0.5% Sep (A2S2). Each treatment was replicated three times in a single plot area of 20 m^2. Three cultivars of maize (*Zea mays* L.) were planted in each treatment: Zhengdan 958 (common cultivar), Liyu 16 (low-accumulation cultivar), and Sanbei 218 (low-accumulation cultivar), which were provided by the Tianjin Luhe Seed Co. The remediation agent was applied evenly to the topsoil (0–20 cm) of each plot using a tillage machine and mixed uniformly. After a 20-day equilibrium period, maize was planted and managed under normal production conditions, including regular weeding, insecticide application, and watering. Maize samples were harvested, dried, and sieved in September 2020. The Cd concentrations of the roots, stems, leaves, and grains of maize were measured. Soil samples were collected from the experimental plots, excluding residues such as gravel, plant roots, and stems. After grinding and air-drying, the samples were passed through 20-, 50-, and 100-mesh nylon sieves to determine the available Cd concentration and fraction of the soil.

Analysis and determination

Soil sample analysis

The total Cd concentration in the soil was determined using HNO_3-HF and the Cd concentration in the digestion solution was determined using ICP-MS (Ultimate 3000-i CAP QC). The available Cd in the soil was extracted using the chelating agent diethylenetriaminepentaacetic acid (DTPA) at a solid-to-liquid ratio of 1:5, and the Cd concentration in the supernatant was determined using ICP-MS after extraction. Quality assurance and control were performed using duplicate samples with three replicates, blanks, and standard reference materials (NIST 2586).

The speciation of Cd in the soil was determined using the Tessier sequential extraction method considering five forms: exchangeable, carbonate-bound, Fe/Mn oxide-bound, organic-bound, and residual. Exchangeable Cd was extracted using $MgCl_2{\cdot}6H_2O$, with a solid-to-liquid ratio of 8:1; carbonate-bound Cd was extracted using NaOAc, with a solid-to-liquid ratio of 8:1; Fe/Mn oxides-bound Cd was extracted using $NH_2OH{\cdot}HCl$, with a solid-to-liquid ratio of 20:1; organic-bound Cd was extracted using HNO_3 and H_2O_2, with a solid-to-liquid ratio of 8:1; and residual Cd was calculated by subtracting the sum of Cd concentration in the first fourth steps from the total soil Cd concentration.

Soil pH was measured using the glass electrode method using a pH meter (HJ 615-2011) (1:2.5 w/v). The sample EC was measured using a conductivity meter (Five Easy Plus; Mettler Toledo) (1:5 w/v). Soil dissolved organic carbon concentration was determined using the potassium dichromate oxidation method (Wang et al. 2018). Catalase activity was determined by potassium permanganate titration (Bandara et al. 2017). Urease activity was determined using indophenol blue colorimetry and that of alkaline phosphatasewas determined using disodium phenyl phosphate colorimetry (Meena et al. 2016).

Determination of Cd concentration in maize

The Cd concentrations of the roots, stems, leaves, and grains of maize were determined using the HNO_3 digestion method. Wheat flour (GBW08503c) was used for quality control and the Cd concentrations in the digested solution were measured using ICP-MS.

Data analysis

All treatments were independently repeated three times and correlation analysis and graphing were performed using SPSS 17.0 and Origin 2018, respectively.

The Cd^{2+} adsorption capacity (q) was calculated as follows:

$$q = \frac{(C_0 - C_t) \times V}{m} \quad (1)$$

where m is the amount of adsorbent material (g); V is the total volume of the solution (L); and C_0 and C_t are

the mass concentration of Cd^{2+} in the solution ($mg{\cdot}L^{-1}$) before adsorption and at adsorption time t, respectively.

The pseudo-first-order kinetic Eq. (2) and pseudo-second-order kinetic Eq. (3) were used to fit the adsorption kinetics of Cd^{2+} on different adsorption materials.

$$q_t = q_e(1-e^{-K_1 t}) \tag{2}$$

$$q_t = \frac{K_2 q_e^2 t}{1+K_2 q_e t} \tag{3}$$

where K_1 is the rate constant (min^{-1}) of the pseudo-first-order kinetic model; t is the adsorption time (min); K_2 is the rate constant of pseudo-second-order kinetic model ($g{\cdot}mg^{-1}{\cdot}min^{-1}$); and q_e and q_t are the Cd^{2+} adsorption capacity ($mg{\cdot}g^{-1}$) at adsorption equilibrium and t, respectively.

The Langmuir and Freundlich models were used for the non-linear fitting of the adsorption isotherm and were calculated using Eqs. (4) and (5), respectively:

$$q_e = \frac{q_m K_L C_e}{1+K_L C_e} \tag{4}$$

$$q_e = K_F C_e^{\frac{1}{n}} \tag{5}$$

where q_e is the equilibrium adsorption capacity ($mg{\cdot}g^{-1}$), C_e is the equilibrium concentration ($mg{\cdot}L^{-1}$), q_m is the saturated adsorption capacity ($mg{\cdot}g^{-1}$), K_L ($L{\cdot}mg^{-1}$) and K_F ($mg{\cdot}g^{-1}{\cdot}L{\cdot}mg^{-1})^{1/n}$ are Langmuir adsorption constants and Freundlich adsorption constants, respectively, and n is a constant that indicates the adsorption strength and varies with the inhomogeneity of the material.

The accumulation and transport of Cd in maize grains were calculated using the bioconcentration factor (BCF) (Eq. (6)) and translocation factor (TF) (Eq. (7)). The translocation factor refers to the transport of heavy metals within the plants. The larger the bioconcentration factor, the faster the plant absorbs heavy metals, and the larger the transport coefficient, the stronger the ability of plants to transport heavy metals from roots to shoots (Wang et al. 2019).

$$\mathrm{BCF} = \frac{C_{\mathrm{grain}}}{C_{\mathrm{soil}}} \tag{6}$$

$$\mathrm{TF} = \frac{C_{\mathrm{grain}}}{C_{\mathrm{root}}} \tag{7}$$

where C_{grain}, C_{root}, and C_{soil} ($mg{\cdot}kg^{-1}$) are the Cd concentrations of maize grains, roots, and soil, respectively.

Results and discussion

Performance of Cd adsorption by rBC, Sep, and rBC + Sep

The fitting curves of the adsorption kinetic models for Cd^{2+} by rBC, Sep, and rBC + Sep are shown in Fig. 1a. The adsorption capacity of the different adsorption materials for Cd^{2+} showed a rapidly increasing pattern (0–120 min) and reached adsorption equilibrium after 120 min. This could be attributed to the presence of abundant adsorption sites on the adsorbent during the initial stage. As the adsorption time increased, the gradual saturation of the available adsorption sites resulted in a decrease in the adsorption rate (Mane and Babu 2013). As shown in Table 2, the pseudo-second-order kinetic fitting R^2 values of the three adsorbents were 0.92, 0.93, and 0.97, respectively, which were higher than those of

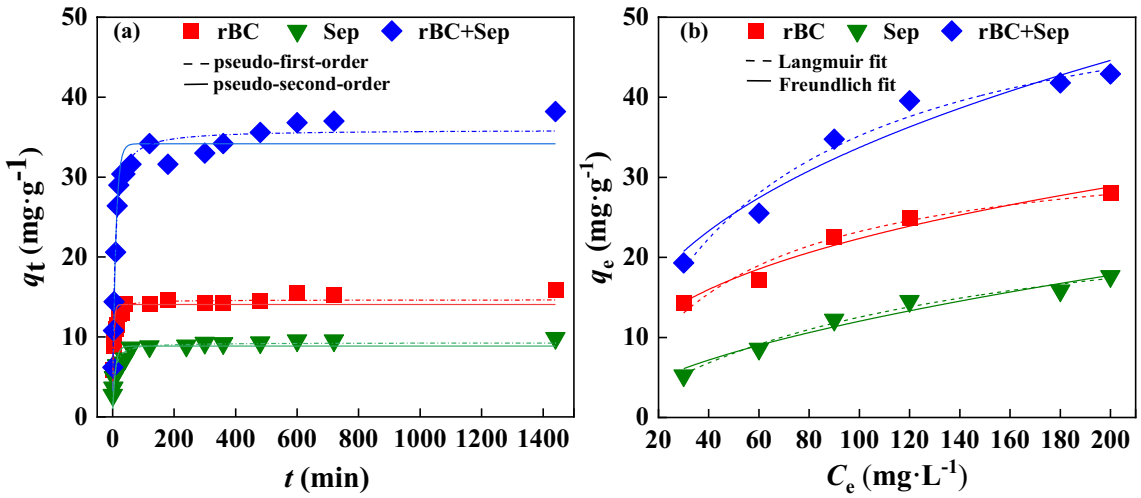

Fig. 1 Adsorption kinetics **a** and adsorption isotherm **b** of Cd^{2+} on rBC, Sep, and rBC + Sep

Table 2 Adsorption kinetic parameters of Cd^{2+} on rBC, Sep, and rBC + Sep

Samples	Quasi-first-order kinetic model			Quasi-second-order kinetic model		
	q_e (mg·g^{-1})	K_1 (min^{-1})	R^2	q_e (mg·g^{-1})	K_2 (g·mg^{-1}·min^{-1})	R^2
rBC	14.05	0.27	0.74	14.65	0.029	0.92
Sep	8.85	0.12	0.80	9.28	0.019	0.93
rBC + Sep	34.17	0.10	0.94	35.92	0.004	0.97

Adsorption capacity of Cd^{2+} at adsorption equilibrium (q_e; mg·g^{-1}), Rate constant of the pseudo-first-order kinetic model (K_1; min^{-1}), Rate constant of the quasi-second-order kinetic model (K_2; g·mg^{-1}·min^{-1})

the pseudo-first-order kinetics. The pseudo-second-order kinetic model better fitted the adsorption process of Cd^{2+} by rBC, Sep, and rBC + Sep, indicating that the adsorption process of Cd^{2+} was mainly chemical.

Langmuir and Freundlich models were used to fit the adsorption isotherm data of Cd^{2+} onto the adsorbent (Fig. 1b), and the fitting parameters are shown in Table 3. The results revealed that the Langmuir isotherm model provided a better fit for the adsorption of Cd^{2+} ($R^2 > 0.97$). This suggests that the adsorption of Cd^{2+} by rBC and Sep primarily involved a uniform adsorption process in a monolayer, which is consistent with the findings of Foo and Hameed (2010). The theoretical maximum adsorption amount of rBC, Sep, rBC + Sep for Cd^{2+} predicted by the Langmuir model was in the order of rBC + Sep (43.53 mg·g^{-1}) > rBC (27.88 mg·g^{-1}) > Sep (17.77 mg·g^{-1}), which agreed with the results of the adsorption kinetics experiment.

Adsorption mechanisms of rBC, Sep, and rBC + Sep on Cd

The surface structure and elemental concentration of the biochar were characterized using SEM–EDS. Figure 2a–c show the rBC and Sep materials before Cd^{2+} adsorption and Fig. 2d–f show the rBC and Sep materials after Cd^{2+} adsorption. rBC before adsorption shows a layered and overlapping shape, with a loose texture and many wrinkles, whereas Sep exhibits a smooth, straight fiber structure. After adsorption, Cd^{2+} appeared uniformly on the surface of the adsorbent, indicating that Cd^{2+} was successfully adsorbed. From a structural perspective, the successful adsorption of Cd^{2+} may be due to the abundant pores and internal cavity structures on the surface of rBC as well as the large smooth surface of Sep. The EDS spectrum analysis revealed that Sep contains a large amount of metal elements and it is tentatively speculated that Cd^{2+} may undergo a chemical reaction with certain metal elements in Sep to form precipitates (Zhang et al. 2019).

The FTIR spectra of rBC, Sep, and rBC + Sep is shown in Fig. 3. A peak at 3427 cm^{-1} was observed in rBC, Sep, and rBC + Sep, which corresponded to the stretching vibration of -OH and adsorption (Chang et al. 2019; Li et al. 2015). The two weak absorption peaks observed at approximately 2916 and 2848 cm^{-1} were attributed to the stretching vibrations of -CH_2 and -CH_3, respectively. The absorption peak at 1432 cm^{-1} was assigned to the stretching vibration of -CH_2. The vibration peak of rBC + Sep shifted to around 1594 cm^{-1}, corresponding to the C = C vibration peak. The characteristic peak at 1018 cm^{-1} was assigned to the stretching vibration of -C-O. Compared to rBC, Sep exhibited a sharper and larger absorption peak at 1201 cm^{-1}, corresponding to the stretching vibration of the C-O bond. The absorption peaks at 875 and 667 cm^{-1} indicated the presence of single and polycyclic compounds. The peak at 464 cm^{-1} was attributed to the bending vibration of the Si-O-Si bond.

Upon the adsorption of Cd^{2+}, the characteristic peaks representing -OH in the biochar decreased from approximately 3427 to 3388 cm^{-1}, indicating a possible reaction between Cd^{2+} and -OH on the biochar surface, leading to the corresponding carbonate or hydroxide precipitation (Xu et al. 2013). Furthermore, an enhancement of the broad peak at 1018 cm^{-1} was observed upon the adsorption of Cd^{2+} following the Sep treatment, suggesting the

Table 3 Isotherm parameters for Cd^{2+}adsorption on rBC, Sep, and rBC + Sep

Samples	Langmuir model			Freundlich model		
	Q_m (mg·g^{-1})	K_L (L·mg^{-1})	R^2	K_F [mg·g^{-1}(L·mg^{-1})$^{1/n}$]	n	R^2
rBC	34.86	0.02	0.96	4.15	0.37	0.96
Sep	28.40	0.01	0.98	6.90	0.56	0.96
rBC + Sep	52.56	0.02	0.97	5.26	0.40	0.94

Saturated adsorption capacity (Q_m; mg·g^{-1}), Langmuir adsorption constant (K_L; L·mg^{-1}), Freundlich adsorption constant [K_F; mg·g^{-1}·(L·mg^{-1})$^{1/n}$], Constant of adsorption strength (n)

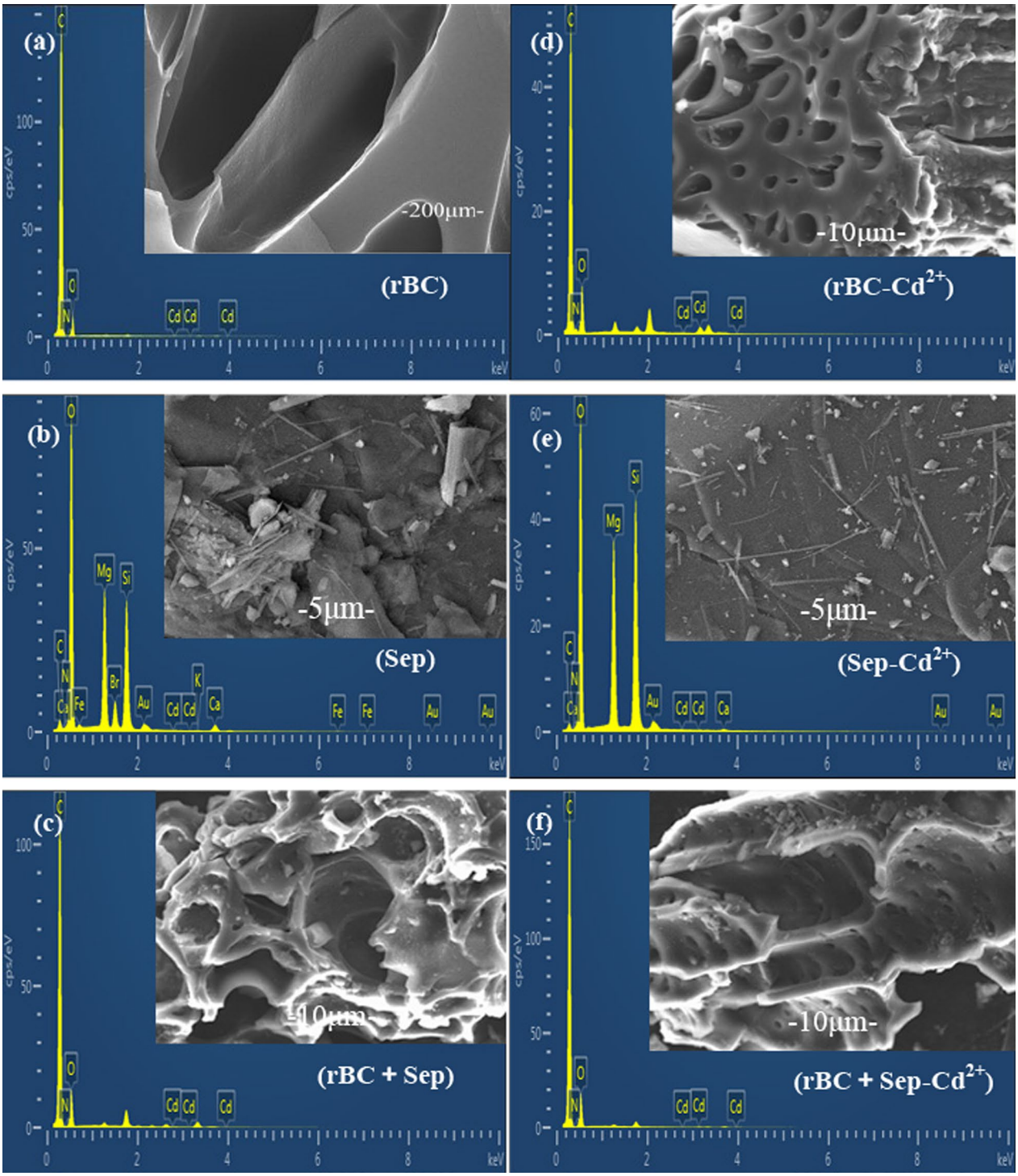

Fig. 2 SEM–EDS image of rBC, Sep, and rBC + Sep before **a**–**c** and after **d**–**f** Cd^{2+} adsorption

potential involvement of Si-O-Si groups on the surface of the Sep in the adsorption of Cd^{2+}.

The XRD analysis of rBC, Sep, and their composite materials revealed a broad diffraction peak of rBC at approximately $2\theta = 25°$, which is a characteristic peak of graphite structure (Fig. 4). The peaks of rBC-Cd at $2\theta = 23.5°$, 30.3°, 36.4°, 43.8°, 49.9°, and 58.2° correspond to crystal planes (012), (104), (110), (202), (116), and (122)

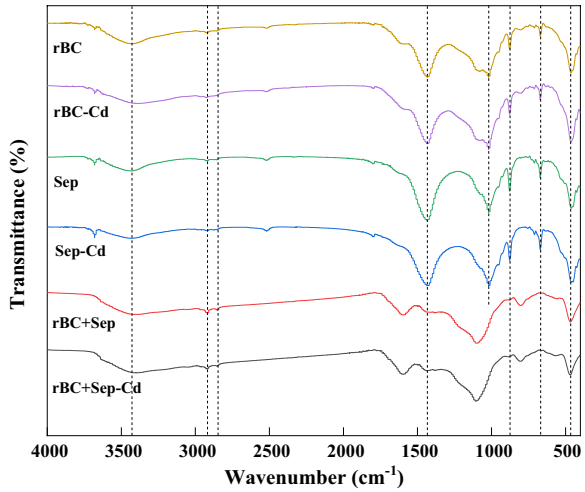

Fig. 3 The FTIR spectra of rBC, Spe and rBC + Spe before and after Cd^{2+} adsorption

of $CdCO_3$, respectively, suggesting that precipitation is the adsorption mechanism of Cd^{2+} on rBC (Fig. 4a). The XRD pattern of Sep showed diffraction peaks at 2θ = 23.0°, 29.4°, 47.5°, and 48.5°, corresponding to crystal planes (012), (104), (018), and (116) of $CaCO_3$, respectively. Compared with that of Sep, the XRD pattern of Sep-Cd showed a new peak at 2θ = 31.7° (Fig. 4b), which was attributed to the crystal plane (-111) of $Cd(OH)_2$, indicating that the precipitation of O–H groups and Cd^{2+} may be one of the mechanisms through which Sep adsorbs Cd^{2+} (Xu et al. 2009). After the adsorption of Cd^{2+} by the composite material of rBC and Sep, the XRD pattern of the composite material showed the characteristic peaks of $CdCO_3$ and $Cd(OH)_2$. Specifically, in the rBC + Sep-Cd material, there were peaks at 2θ = 23.5°, 36.4°, 47.5°, and 48.5°, corresponding to crystal planes (012), (110), (018), and (116) of $CdCO_3$, respectively, and a peak at 2θ = 31.7°, corresponding to the crystal plane (-111) of $Cd(OH)_2$. This indicated that carbonate precipitation occurred during the adsorption of Cd^{2+} by rBC + Sep (Fig. 4c).

Effects of rBC, Sep, and rBC + Sep on available Cd concentration and Cd fractions in soil

As shown in Fig. 5, the application of rBC, Sep, and rBC + Sep resulted in a decrease in the soil available Cd concentration with an increase in the amount of adsorbent applied compared to the CK treatment. Therefore, passivating agents play a crucial role in reducing the soil Cd concentration. In the single material adsorption, the available Cd concentration of soil treated with A2 and S2 decreased by 25.88% and 34.54%, respectively, compared with CK. In the combined treatment, the available Cd concentration in the soil treated with A2S2 was the lowest, showing a 38.24% reduction compared with CK (p < 0.05).

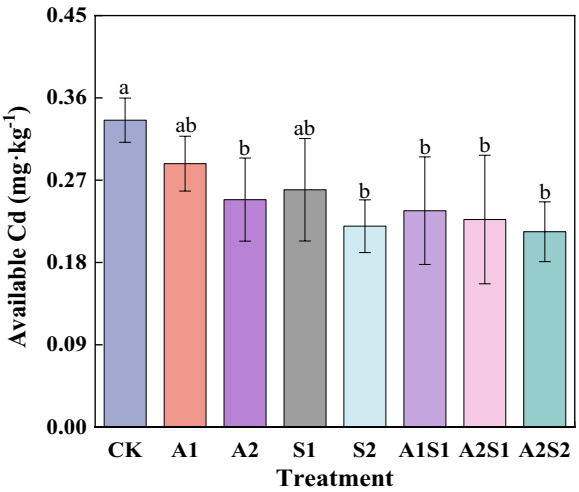

Fig. 5 Soil available Cd concentration under different treatments. Different letters show significant differences (p < 0.05)

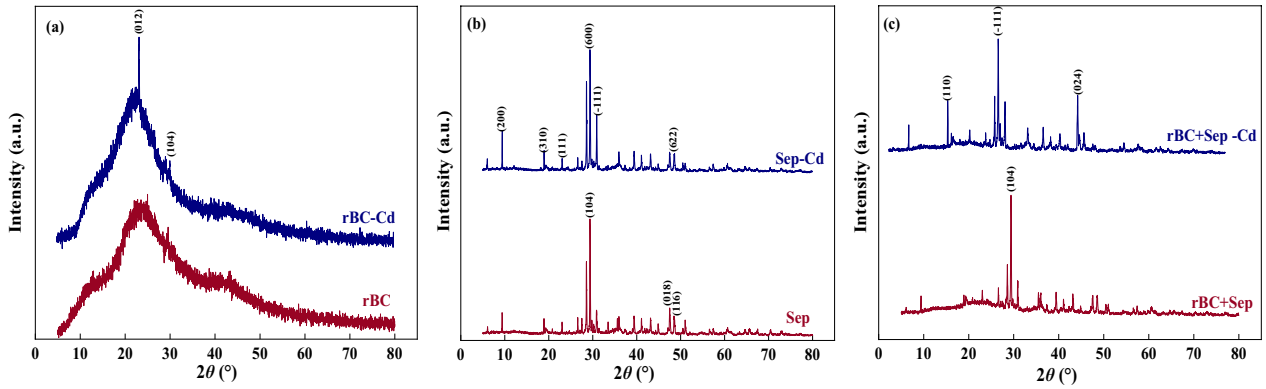

Fig. 4 The XRD patterns of rBC (**a**), Sep (**b**) and rBC + Sep (**c**) before and after Cd^{2+} adsorption

For the distribution of heavy metal forms, exchangeable and carbonate-bound states are considered to be biologically available, whereas residual states are considered to be the most stable and least biologically available form (Lock et al. 2003). In soil without the application of passivating agents, the predominant forms of Cd were the Fe/Mn oxide-bound state (35.24%) and the exchangeable state (28.30%), with the residual state accounting for only 6.45% and possessing some potential biological availability (Fig. 6), consistent with the findings of Zhang et al. (2020). The application of passivating agents decreased the proportion of exchangeable Cd in the soil to varying degrees, with the decreasing range increasing with the amount of passivating agent applied, ranging from 24.33 to 34.73%. Compared to CK, the exchangeable Cd decreased by 26.60% and 28.97%, respectively, when rBC was applied alone. This is because rBC has a porous carbon framework structure with clear and distinct pore profiles that can more effectively adsorb and retain heavy metals in the soil, thereby reducing their biological availability (Beesley et al. 2011). Compared to the application of rBC alone, S2 achieved the largest decrease in exchangeable Cd at 34.73%. Thawornchaisit and Polprasert (2009) found that different passivating agents had different effects on soil remediation efficiency, which is consistent with the results of this study. Furthermore, the proportion of carbonate-bound Cd decreased to varying degrees. The proportion of carbonate-bound Cd accounted for 25.44% without passivation treatment but decreased by 19.82% to 23.53% following passivation treatment. The reduction was smaller when rBC and Sep were applied separately, decreasing by 0.02–0.06 units. When 0.2% rBC and 0.5% Sep were applied simultaneously, the proportion of carbonate-bound Cd decreased to 19.96%. After passivation treatment, the available Cd concentration in the soil decreased, gradually transforming from exchangeable and carbonate-bound forms to Fe/Mn oxides and residual forms, resulting in reduced mobility and bioavailability (Seshadri et al. 2017). This finding was consistent with the results of the present study. In this study, the Fe/Mn oxide-bound Cd increased to varying degrees (3.89% to 10.71%) following passivation treatment. The proportion of Fe/Mn oxide-bound Cd in the CK treatment was 35.24%, and the differences under different application rates were not significant ($p > 0.05$). The passivation treatment effectively increased the proportion of residual Cd. The passivation treatment effectively increased the proportion of residual Cd by 115.45–294.20%. Uchimiya et al. (2010) also showed that the input of biochar promoted the transformation of exchangeable Cd into residual forms, possibly because residual heavy metals are generally composed of primary and secondary silicates, sulfides, and other stable secondary minerals. In addition, biochar input increases soil pH and available silicon concentration, leading to the formation of new, structurally stable silicate precipitates with soil heavy metal ions and silicate ions, thereby increasing the proportion of residual forms (Neumann and zur Nieden 2001).

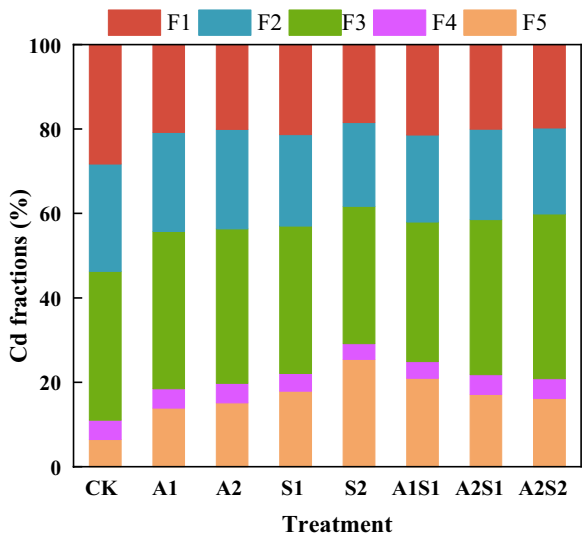

Fig. 6 Soil Cd fractions under different treatments. Exchangeable (F1), Carbonate-bound (F2), Fe/Mn oxides-bound (F3), Organic (F4), Residual (F5)

Effects of rBC, Sep, and rBC + Sep on Cd concentration in maize

Figure 7 depicts the impact of rBC and Sep treatments on Cd accumulation in various parts of the three maize cultivars. The Cd accumulation pattern was in the order of roots > leaves > stems > grains. Following the application of the passivation agents to the soil, a significant reduction in Cd concentration was observed in all parts of the maize plants. The range of Cd reduction in the roots of Liyu 16 varied from 9.66 to 32.77%. The decrease in Liyu 16 was the largest, although it was not statistically different from that in the two other cultivars ($p > 0.05$). However, a significant reduction in Cd concentration was observed in the roots of Zhengdan 958 and Sanbei 218 ($p < 0.05$). Under 0.2% rBC + 0.5% Sep, the maximum reductions in Cd concentration were 40.04% and 46.07% in the roots of Zhengdan 958 and Sanbei 218, respectively. A significant reduction in Cd content was also observed in the stems of all three maize cultivars ($p < 0.05$), with the reduction increasing with increasing passivation concentration. The reduction in Cd concentration in the stems of Liyu 16, Zhengdan 958, and Sanbei 218 ranged from 10.27–40.47%, 3.12–36.53%, and 6.60–53.60%, respectively. In the leaves of Zhengdan 958,

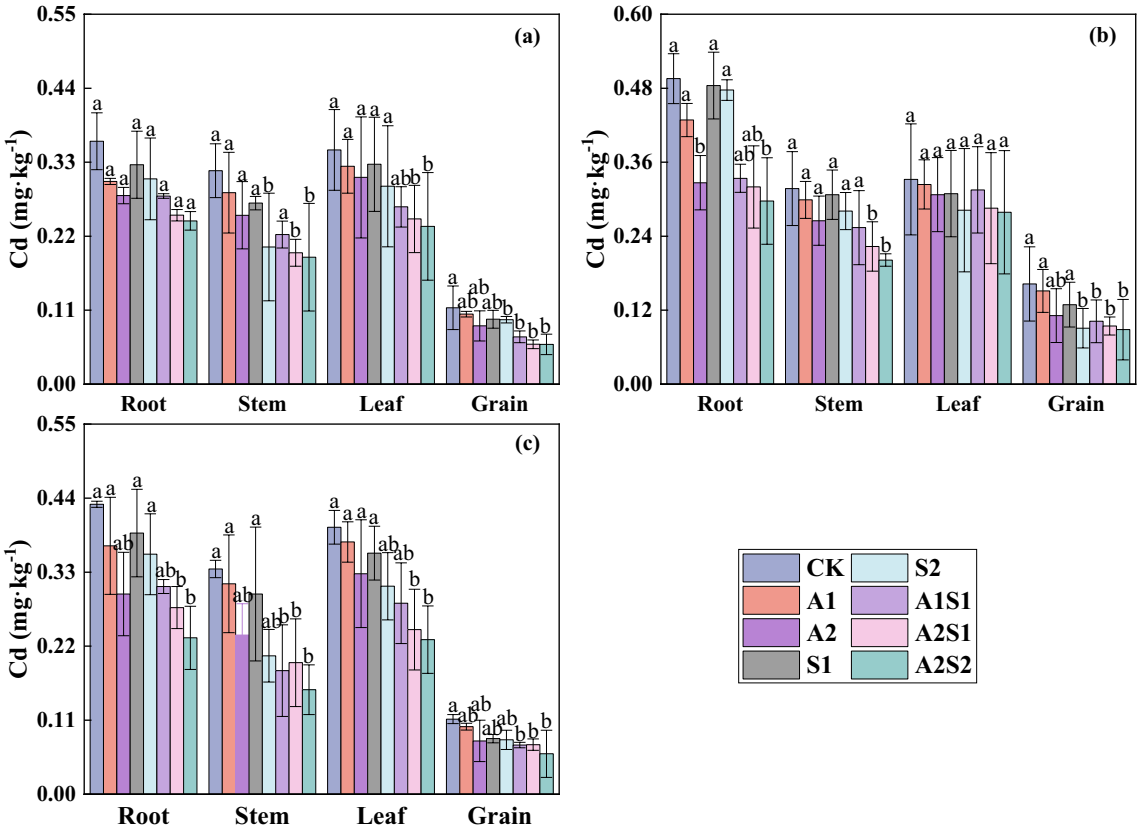

Fig. 7 Effects of different treatments on Cd concentration of different parts of maize for different cultivars. (**a**): Liyu 16, (**b**): Zhengdan 958, (**c**): Sanbei 218. Error bars represent ± SE (n = 3). Different letters show significant differences ($p < 0.05$)

A2S2 treatment decreased Cd concentration by 16.05%, which was an insignificant reduction in Cd concentration ($p > 0.05$) compared with CK treatment. However, a significant reduction in Cd concentration was observed in the leaves of Liyu 16 and Sanbei 218 ($p < 0.05$), with maximum reductions of 32.62% and 42.10%, respectively.

In this experiment, the accumulation of Cd in grains of the three cultivars of maize in the CK exceeded the Cd limit of ≤ 0.1 mg·kg^{-1} set by the China's National Food Safety Standard – Maximum Levels for Contaminants in Foods (GB2762-2022). Following the application of passivation agents, a significant reduction in Cd concentration was observed in the grains of all three maize cultivars ($p < 0.05$), with reductions of 13.80% to 31.40% observed in the grains of Zhengdan 958. Under A2S2 treatment, the Cd concentration in the grains of Liyu 16, Zhengdan 958 and Sanbei 218 decreased by 47.85%, 45.61% and 46.15%, respectively, indicating that the application of 0.2% rBC + 0.5% Sep passivation material had the greatest inhibitory effect on Cd in the grains of Liyu 16, which may be attributed to the different genotypes and tolerance mechanisms of the same plant species. Further studies are needed to elucidate the underlying mechanism (Bhargava et al. 2012). The Cd concentration in the grain of the low-accumulating cultivar Liyu 16 was lower than 0.1 mg·kg^{-1} (except for S1 treatment) after treatment, which met the standard. However, under A1, S1, S2, and A1S1 treatments of the common cultivar Zhengdan 958 and the S1 treatment of the low-accumulating cultivar Sanbei 218, the Cd concentration in the grain was above 0.1 mg·kg^{-1}. Among them, the most effective treatment for reducing Cd concentration in grains was A2S2 treatment, which showed reductions of 47.85%, 45.61%, and 46.15% compared to CK. The combined treatment of rBC + Sep effectively reduced the Cd concentration in grains, which met the requirements of the above standards.

Effects of rBC, Sep, and rBC + Sep on transport ability of Cd in maize

We evaluated the ability of plants to accumulate and transport the Cd using bioconcentration and translocation factors (Cui et al. 2017). The Cd bioconcentration factors of the two low-accumulating maize cultivars, Liyu 16 and Sanbei 218, were significantly lower than that of the common cultivar Zhengdan 958 (Fig. 8a).

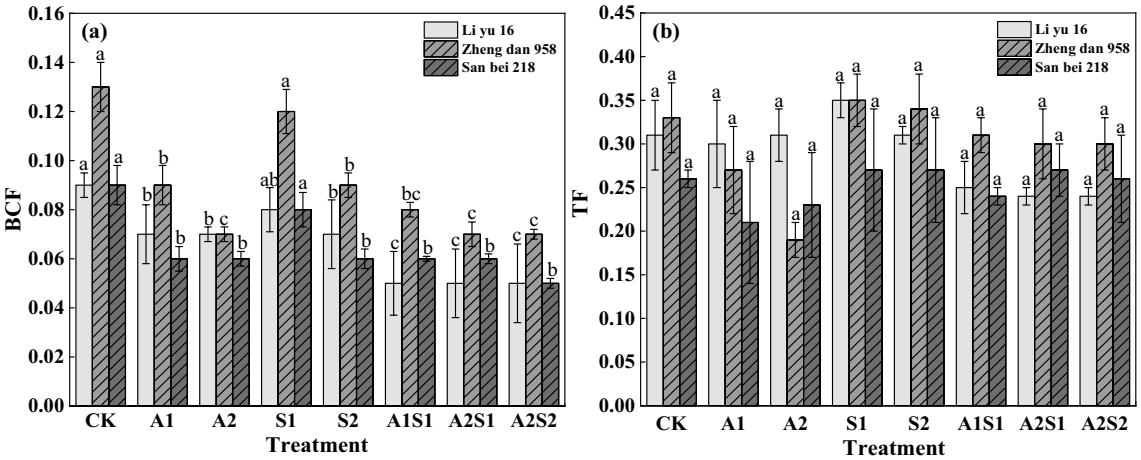

Fig. 8 The bioconcentration (**a**) and translocation factors (**b**) of Cd for different treatments. Different letters show significant differences ($p<0.05$)

This finding was consistent with that of Wu et al. (2005), who found differences in Cd absorption, transport, and accumulation among different wheat genotypes. This phenomenon may be attributed to the genetic regulation of Cd accumulation in crops, which is closely associated with the ability of different cellular organelles in the roots, stems, and leaves to fix, store, and tolerate Cd, as well as the influence of genes involved in Cd regulation (Yue et al. 2018; Feng et al. 2020). Moreover, after applying the passivator, the Cd bioconcentration factor in the grains of the three maize cultivars significantly decreased ($p<0.05$). In Liyu 16, the bioconcentration factor of Cd in grains decreased by 2.89–20.37% compared to the CK. The Cd bioconcentration factor in Zhengdan 958 ranged from 0.07 to 0.13, with a mean of 0.09. In Sanbei 218, under the A2S2 treatment, the Cd bioconcentration factor decreased significantly by 17.71% compared with CK ($p<0.05$). Variance in heavy metal uptake and adaptation capabilities among different maize cultivars may be attributed to various factors, including differential gene expressions within the crop and disparities in the application of passivating agents (Feng et al. 2020; Guo et al. 2018).

A higher translocation factor indicates a stronger ability of the heavy metal to transfer from the roots to the aboveground parts (Sun et al. 2008). Zhi et al. (2014) suggested that the criteria for screening low-accumulating crop cultivars must satisfy both the bioconcentration and translocation factors of the cultivar of less than 1. In this study, the Cd translocation factor of the three maize cultivars from roots to the grains was less than 1 (Fig. 8b), indicating that Cd mainly accumulated in the roots of maize. In Liyu 16, the Cd translocation factor from roots to grains ranged from 0.24 to 0.35, with a mean of 0.29. In Zhengdan 958, the Cd translocation factor ranged from 0.19 to 0.35, with a mean of 0.30. In Sanbei 218, the Cd translocation factor ranged from 0.21 to 0.27, with a mean of 0.25. These findings indicated that the Cd transferred from the soil to the grains was very low and most of the Cd was intercepted by the roots, stems, and leaves. Due to the decrease of Cd concentration in different parts of maize under the treatment of adding passivating agent, it is feasible to use passivating agent to repair Cd-contaminated farmlands.

Influence of soil chemical properties and enzyme activities under different treatments

As shown in Table4, the application of rBC + Sep resulted in a moderate increase in soil pH compared to CK but the differences were insignificant ($p>0.05$). The magnitude of the increase generally increased with the application of passivating agents, with a pH increasing by 0.17 under A2S2 treatment. Compared with CK, except for S1 treatment, soil electrical conductivity under each treatment increased to varying degrees but the differences were

Table 4 Effects of different treatments on basic properties of soil

Treatment	pH	EC (μS·cm^{-1})	DOC (mg·kg^{-1})
CK	8.34 ± 0.12b	265.9 ± 63.3a	93.96 ± 18.00b
A1	8.34 ± 0.15b	272.5 ± 58.3a	100.45 ± 10.94ab
A2	8.35 ± 0.12b	293.7 ± 63.9a	111.73 ± 26.51a
S1	8.53 ± 0.08a	260.3 ± 57.0a	105.99 ± 22.44ab
S2	8.43 ± 0.17ab	316.4 ± 96.8a	106.58 ± 14.96ab
A1S1	8.47 ± 0.21ab	305.4 ± 59.9a	104.76 ± 18.04ab
A2S1	8.38 ± 0.19ab	332.6 ± 101.5a	101.92 ± 12.12ab
A2S2	8.50 ± 0.14ab	278.7 ± 73.5a	107.38 ± 12.08ab

Electric conductivity (EC; μS·cm^{-1}), Dissolved organic carbon (DOC; mg·kg^{-1}), Data are shown as mean ± standard deviation ($n=3$), Different letters in columns indicate significant differences ($p<0.05$)

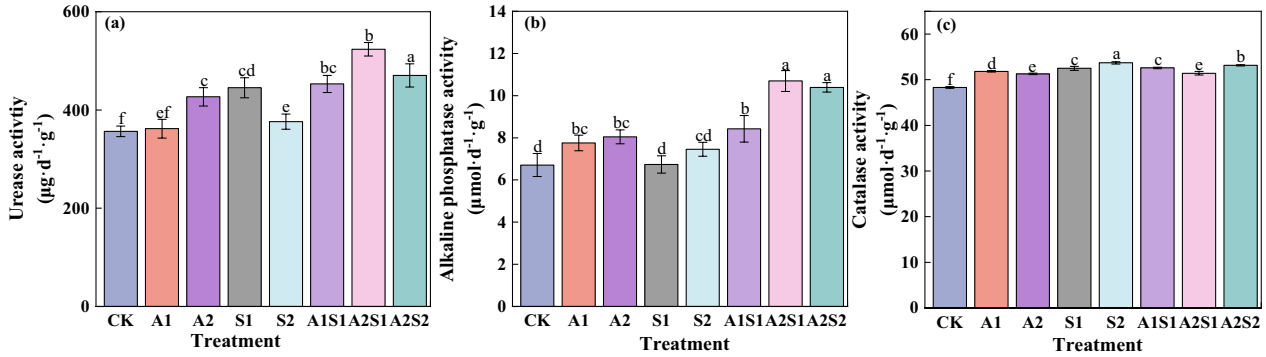

Fig. 9 Effects of different treatments on soil urease (**a**), alkaline phosphatase (**b**) and catalase (**c**) activities. Different letters show significant differences ($p < 0.05$)

insignificant ($p > 0.05$). When the application rates of rBC and Sep were 0.2% and 0.2%, the electrical conductivity increased by 25.10%. Except for under A2, soil dissolved organic carbon concentration showed no significant difference compared to CK (except for S1, $p > 0.05$), with increases of 6.91–14.28%.

Soil enzyme activity, as an organic component of the soil, is involved in the transformation of substances and energy in the soil, thereby affecting soil metabolism (Jimenez et al. 2002). Soil enzymes are sensitive to heavy metals (Zhang et al. 2015) and their activity is affected to varying degrees when exposed to heavy metal stress. In this study, after the application of different rates of rBC and Sep, the activities of urease, alkaline phosphatase, and catalase in the soil increased to varying degrees compared to CK. Urease activity exhibited an initial increase and subsequent decrease when rBC and Sep were applied in combination. When the Sep application rate was 0.2% and the rBC application rate was 0.2%, the activity of soil urease was higher than that at an application rate of 0.1% for Sep. However, when the Sep application rate increased to 0.5%, the activity of urease decreased. Under A2S1, the activity of soil urease increased significantly by 46.86% ($p < 0.05$) compared to CK (Fig. 9a). Under A2S1 and A2S2, the activity of soil alkaline phosphatase increased significantly by 3.99 and 3.68 units, respectively ($p < 0.05$) (Fig. 9b). Application of various concentrations of passivators induced an increase in catalase activity by 6.16–11.20%. Notably, the highest catalase activity was achieved when a rate of 0.5% Sep was applied, exhibiting a significant difference compared to that of CK ($p < 0.05$) (Fig. 9c).

Conclusion

Pseudo-second-order kinetic and Langmuir models could well explain the adsorption process of Cd by rBC, Sep, and rBC + Sep, indicating that the adsorption of Cd^{2+} was mainly chemical. The combined application of rBC and Sep significantly reduced the concentration of DTPA-Cd in the soil, which tended to change from a more active exchangeable and carbonate-bound state to a more stable residual and Fe/Mn oxidation-bound state. In addition, Cd concentrations in roots, stems, leaves and grains of Liyu 16, Sanbei 218 and Zhengdan 958 were decreased under different passivator treatments. The application of single and composite materials can increase soil enzyme activity, as well as soil pH and electrical conductivity, but the differences for the latter two were not significant. Therefore, it is recommended to apply 0.2% rBC + 0.5% Sep combined material in weakly alkaline Cd-contaminated soil.

Acknowledgements
Not applicable.

Author contributions
YZ: Data curation, Writing-original draft. SG: Methodology, Investigation. HJ: Supervision. TS: Validation. SZ: Writing-review & editing. SW: Investigation. YS: Validation, Project administration, Funding acquisition.

Funding
This work was supported by the Innovation Program of Chinese Academy of Agricultural Sciences (CAAS-CSGLCA-202302), and the National Natural Science Foundation of China (31971525).

Availability of data and materials
Data are available upon reasonable request.

Declarations

Ethics approval and consent to participate
Not applicable.

Consent for publication
All authors agreed and approved the manuscript for publication in *Ecological Processes*.

Competing interests
The authors declare that they have no competing interest.

Received: 27 September 2023 Accepted: 16 November 2023
Published online: 09 January 2024

References

Abad-Valle P, Álvarez-Ayuso E, Murciego A, Pellitero E (2016) Assessment of the use of sepiolite amendment to restore heavy metal polluted mine soil. Geoderma 280:57–66.https://doi.org/10.1016/j.geoderma.2016.06.015

Ahmad M, Rajapaksha AU, Lim JE, Zhang M, Bolan N, Mohan D, Vithanage M, Lee SS, Ok YS (2014) Biochar as a sorbent for contaminant management in soil and water: A review. Chemosphere 99:19–33.https://doi.org/10.1016/j.chemosphere.2013.10.071

Bandara T, Herath I, Kumarathilaka P, Seneviratne M, Seneviratne G, Rajakaruna N, Vithanage M, Ok YS (2017) Role of woody biochar and fungal-bacterial co-inoculation on enzyme activity and metal immobilization in serpentine soil. J Soils Sediments 17:665–673.https://doi.org/10.1007/s11368-015-1243-y

Basta NT, McGowen SL (2004) Evaluation of chemical immobilization treatments for reducing heavy metal transport in a smelter-contaminated soil. Environ Pollut 127:73–82.https://doi.org/10.1016/s0269-7491(03)00250-1

Beesley LK, Moreno-Jimenez E, Gomez-Eyles JL, Harris E, Robinson B, Sizmur T (2011) A review of biochars' potential role in the remediation, revegetation and restoration of contaminated soils. Environ Pollut 159:3269–3282.https://doi.org/10.1016/j.envpol.2011.07.023

Bhargava A, Carmona FF, Bhargava M, Srivastava S (2012) Approaches for enhanced phytoextraction of heavy metals. J Environ Manage 105:103–120.https://doi.org/10.1016/j.jenvman.2012.04.002

Chang RH, Sohi SP, Jing FQ, Liu YY, Chen JW (2019) A comparative study on biochar properties and Cd adsorption behavior under effects of ageing processes of leaching, acidification and oxidation. Environ Pollut 254:113123.https://doi.org/10.1016/j.envpol.2019.113123

Cheng S, Chen T, Xu WB, Huang J, Jiang SJ, Yan B (2020) Application research of biochar for the remediation of soil heavy metals contamination: a review. Molecules 25:3167. https://doi.org/10.3390/molecules25143167

Covelo EF, Vega FA, Andrade ML (2007) Simultaneous sorption and desorption of Cd, Cr, Cu, Ni, Pb, and Zn in acid soils: I. Selectivity sequences. J Hazard Mater 147:852–861.https://doi.org/10.1016/j.jhazmat.2007.01.123

Cui JH, Liu TX, Li FB, Yi JC, Liu CP, Yu HY (2017) Silica nanoparticles alleviate cadmium toxicity in rice cells: Mechanisms and size effects. Environ Pollut 228:363–369.https://doi.org/10.1016/j.envpol.2017.05.014

Fan J, Cai C, Chi HF, Reid BJ, Coulon F, Zhang YC, Hou YW (2020) Remediation of cadmium and lead polluted soil using thiol-modified biochar. J Hazard Mater 388:122037.https://doi.org/10.1016/j.jhazmat.2020.122037

Feng TY, He XL, Zhuo RY, Qiao GR, Han XJ, Qiu WM, Chi LF, Zhang DY, Liu MY (2020) Identification and functional characterization of ABCC transporters for Cd tolerance and accumulation in *Sedum alfredii* Hance. Sci Rep 10:20928.https://doi.org/10.1038/s41598-020-78018-6

Foo KY, Hameed BH (2010) Insights into the modeling of adsorption isotherm systems. Chem Eng J 156:2–10.https://doi.org/10.1016/j.cej.2009.09.013

Guo FY, Ding CF, Zhou ZG, Huang GX, Wang XX (2018) Stability of immobilization remediation of several amendments on cadmium contaminated soils as affected by simulated soil acidification. Ecotoxicol Environ Saf 161:164–172.https://doi.org/10.1016/j.ecoenv.2018.05.088

Jimenez MDLP, Horra AMDL, Pruzzo L, Palma RM (2002) Soil quality: a new index based on microbiological and biochemical parameters. Biol Fertil Soils 35:302–306.https://doi.org/10.1007/s00374-002-0450-z

Li FF, Dai YZ, Gong M, Yu TP, Chen XJ (2015) Synthesis, characterization of magnetic-sepiolite supported with TiO_2, and the photocatalytic performance over Cr(VI) and 2,4-dichlorophenol co-existed wastewater. J Alloys Compd 638:435–442.https://doi.org/10.1016/j.jallcom.2015.03.070

Liang XF, Han J, Xu YM, Sun YB, Wang L, Tan X (2014) In situ field-scale remediation of Cd polluted paddy soil using sepiolite and palygorskite. Geoderma 235–236:9–18.https://doi.org/10.1016/j.geoderma.2014.06.029

Lock K, Janssens F, Janssen CR (2003) Effects of metal contamination on the activity and diversity of springtails in an ancient Pb-Zn mining area at Plombières, Belgium. Eur J Soil Biol 39:25–29.https://doi.org/10.1016/s1164-5563(02)00006-7

Mane VS, Babu PVV (2013) Kinetic and equilibrium studies on the removal of Congo red from aqueous solution using Eucalyptus wood (*Eucalyptus globulus*) saw dust. J Taiwan Inst Chem Eng 44:81–88.https://doi.org/10.1016/j.jtice.2012.09.013

Meena MD, Joshi PK, Jat HS, Chinchmalatpure AR, Narjary B, Sheoran P, Sharma DK (2016) Changes in biological and chemical properties of saline soil amended with municipal solid waste compost and chemical fertilizers in a mustard-pearl millet cropping system. Catena 140:1–8.https://doi.org/10.1016/j.catena.2016.01.009

Neumann D, zur Nieden U (2001) Silicon and heavy metal tolerance of higher plants. Phytochemistry 56:685–692.https://doi.org/10.1016/S0031-9422(00)00472-6

Seshadri B, Bolan NS, Choppala G, Kunhikrishnan A, Sanderson P, Wang H, Currie LD, Tsang D, Ok YS, Kim G (2017) Potential value of phosphate compounds in enhancing immobilization and reducing bioavailability of mixed heavy metal contaminants in shooting range soil. Chemosphere 184:197–206.https://doi.org/10.1016/j.chemosphere.2017.05.172

Song ZG, Tang SR, Ding YZ, Feng RW, Zhang CB (2011) Effects of different amendments on cadmium uptake by maize under field conditions. J Agro Environ Sci 30:2152–2159

Sun YB, Zhou QX, Diao CY (2008) Effects of cadmium and arsenic on growth and metal accumulation of Cd-hyperaccumulator *Solanum nigrum* L. Bioresour Technol 99:1103–1110.https://doi.org/10.1016/j.biortech.2007.02.035

Sun K, Miao CB, He Y (2017) Prospects for the utilization of biochar on remediating soils polluted by heavy metal. Biomass Chem Eng 51:66–74

Thawornchaisit U, Polprasert C (2009) Evaluation of phosphate fertilizers for the stabilization of cadmium in highly contaminated soils. J Hazard Mater 165:1109–1113.https://doi.org/10.1016/j.jhazmat.2008.10.103

Uchimiya M, Lima IM, Thomas Klasson K, Chang S, Wartelle LH, Rodgers JE (2010) Immobilization of heavy metal ions (Cu^{II}, Cd^{II}, Ni^{II}, and Pb^{II}) by broiler litter-derived biochars in water and soil. J Agric Food Chem 58:5538–5544.https://doi.org/10.1021/jf9044217

Wang K, Liu YH, Song ZG, Wang D, Qiu WW (2019) Chelator complexes enhanced *Amaranthus hypochondriacus* L. phytoremediation efficiency in Cd-contaminated soils. Chemosphere 237:124480.https://doi.org/10.1016/j.chemosphere.2019.124480

Wang H, Liu SR, Zhang X, Mao QG, Li XZ, You YM, Wang JX, Zheng MH, Zhang W, Lu XK, Mo JM (2018) Nitrogen addition reduces soil bacterial richness, while phosphorus addition alters community composition in an old-growth N-rich tropical forest in southern China. Soil Biol Biochem 127:22–30. https://doi.org/10.1016/j.soilbio.2018.08.022

Wu FB, Dong J, Qian QQ, Zhang GP (2005) Subcellular distribution and chemical form of Cd and Cd-Zn interaction in different barley genotypes. Chemosphere 60:1437–1446.https://doi.org/10.1016/j.chemosphere.2005.01.071

Xiao X, Chen BL, Chen ZM, Zhu LZ, Schnoor JL (2018) Insight into multiple and multilevel structures of biochars and their potential environmental applications: a critical review. Environ Sci Technol 52:5027–5047.https://doi.org/10.1021/acs.est.7b06487

Xie S (2020) Study on Remediation Effects and Mechanisms of Cadmium Pollution using Modified Sepiolite. Dissertation, Argo-Environmental Protection Institute.

Xu YM, Liang XF, Sun GH, Sun Y, Qin X, Wang L (2009) Surface chemical characteristics of sepiolites and their adsorption mechanisms of Pb^{2+}, $Cd^{2+}$and Cu^{2+}. J Agro Environ Sci 28:2057–2063

Xu XY, Cao XD, Zhao L, Wang HL, Yu HR, Gao B (2013) Removal of Cu, Zn, and Cd from aqueous solutions by the dairy manure-derived biochar. Environ Sci Pollut Res Int 20:358–368.https://doi.org/10.1007/s11356-012-0873-5

Yue JY, Wei XJ, Wang HZ (2018) Cadmium tolerant and sensitive wheat lines: their differences in pollutant accumulation, cell damage, and autophagy. Biol Plant 62:379–387.https://doi.org/10.1007/s10535-018-0785-4

Zhang J, Liu J, Liu RL (2015) Effects of pyrolysis temperature and heating time on biochar obtained from the pyrolysis of straw and lignosulfonate. Bioresour Technol 176:288–291.https://doi.org/10.1016/j.biortech.2014.11.011

Zhang JH, Lu MY, Wan J, Sun YH, Lan HX, Deng XY (2018) Effects of pH, dissolved humic acid and Cu^{2+} on the adsorption of norfloxacin on montmorillonite-biochar composite derived from wheat straw. Biochem Eng J 130:104–112.https://doi.org/10.1016/j.bej.2017.11.018

Zhang LK, Liu XY, Huang XM, Wang WD, Sun P, Li YM (2019) Adsorption of Pb^{2+} from aqueous solutions using Fe-Mn binary oxides-loaded biochar: kinetics, isotherm and thermodynamic studies. Environ Technol 40:1853–1861.https://doi.org/10.1080/09593330.2018.1432693

Zhang JJ, Zhu SG, Zhu LN, Liu HT, Yang JK, Hua DL (2020) Effects of different amendments on ractions and uptake by winter wheat in slightly alkaline soil contaminated by cadmium and nickel. Environ Sci 41:460–468.https://doi.org/10.13227/j.hjkx.201907110
Zhang L, Tang C, Yu HY, Li TX, Zhang XZ, Huang HG (2023) In-situ remediation effect of cadmium-polluted agriculture land using different amendments under rice-wheat rotation. Environ Sci 44:1698–1705
Zhao FJ, Ma Y, Zhu YG, Tang Z, McGrath SP (2015) Soil contamination in China: current status and mitigation strategies. Environ Sci Technol 49:750–759.https://doi.org/10.1021/es5047099
Zhi Y, Sun T, Zhou QX (2014) Assessment of lead tolerance in 23 Chinese soybean cultivars and the effect of lead on their mineral ion complement. Environ Sci Pollut Res 21:12909–12921.https://doi.org/10.1007/s11356-014-3181-4
Zhou JJ, Zhou J, Feng RG (2014) Status of China's heavy metal contamination in soil and its remediation strategy. Bull Chin Acad Sci 29:315–320.https://doi.org/10.3969/j.issn.1000-3045.2014.03.008

Publisher'sNote